

## MNDO Study of the Dimerization of Borane

Wing-Kwong Ip and Wai-Kee Li\*

Department of Chemistry, The Chinese University of Hong Kong, Shatin, N. T.,  
Hong Kong

Received April 4, 1983

The dimerization of borane has been investigated with the MNDO method. Three pathways have been studied by imposing different symmetry restrictions:  $C_{2h}$  symmetry, least-motion, and with no symmetry at all. The activation energies of the three pathways are 3.8, 31.5, and 2.7 kcal/mol, respectively. In view of the known tendency of MNDO to yield high energy for transition states, the low activation energy of the last pathway *probably* means that the dimerization has no or a very small energy barrier. Moreover, it turns out that  $C_s$  symmetry is retained automatically for this pathway.

### INTRODUCTION

Borane,  $BH_3$ , unlike its trisubstituted halo-derivatives  $BX_3$ , exists in dimeric form. This is probably due to the lack of back donation to the empty  $p$  orbital of boron and to the partial positive charge on the boron atom. The equilibrium between two  $BH_3$  units and the  $B_2H_6$  species is exceptionally favorable to the dimeric form. The presence of any measurable concentration of free  $BH_3$  in equilibrium with diborane at elevated temperatures has apparently never been detected<sup>1</sup>, though the  $BH_3^+$  ion has been detected from low pressure pyrolysis of  $B_2H_6$  by mass spectrometry<sup>2</sup>.

The  $sp^2$  hybridized  $BH_3$  self-associates with high efficiency and requires no activation energy and the absolute rate has been measured<sup>2</sup>. The hybridization scheme for  $B_2H_6$  suggested by Hamilton<sup>3</sup> is that two  $sp^2$  hybrid orbitals of boron bond to two terminal hydrogens, while the third  $sp^2$  orbital combines with the remaining  $p$  orbital to form two equivalent hybrid orbitals directed toward the two bridging hydrogens.

In the present work, three pathways of the dimerization processes are studied using the semi-empirical MNDO method. These are: the pathway with  $C_{2h}$  symmetry, the pathway of least-motion, and the pathway with no symmetry constraint.

### METHOD OF CALCULATION

All the calculations in this study make use of the MNDO approximation<sup>4</sup>, which has proven to be satisfactory for boron compounds.<sup>5,6</sup> The disadvantages and strong points of this approximation for boron systems have been discussed by Dewar<sup>5</sup>.

\* Author for correspondence.

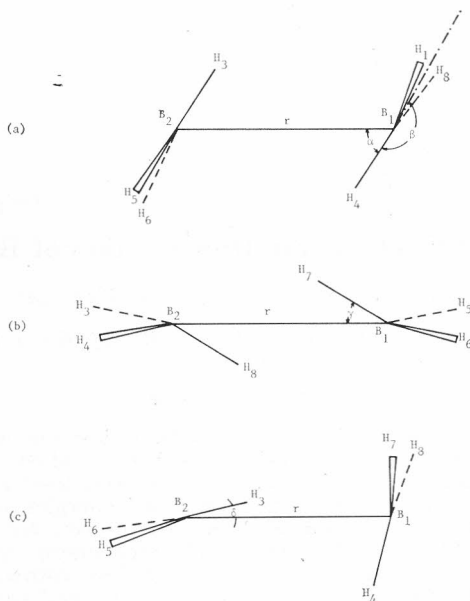


Figure 1. The geometry arrangements and the numbering of atoms for the three dimerization pathways: (a)  $C_{2h}$  pathway, (b) least-motion pathway and (c) pathway with no symmetry constraint.

Figure 1 depicts the three dimerization paths pictorially, along with the numbering of atoms. In the first path,  $C_{2h}$  symmetry is assumed. Specifically, atoms  $B_1$ ,  $B_2$ ,  $H_3$  and  $H_4$  remain co-planar throughout. The second, least-motion path also has  $C_{2h}$  symmetry. However, in this case atoms  $B_1$ ,  $B_2$ , and  $H_3, \dots, H_6$  remain co-planar throughout. In the last path no symmetry restraint is imposed.

In all the calculations the  $B_1$ — $B_2$  distance (denoted as  $r$ ) is taken as the reaction coordinate. For every fixed value of  $r$ , aside from any symmetry conditions specified, all other structural parameters are varied until minimum energy for the system is obtained.

In the calculation of the first two pathways the transition state is taken as the point of maximum energy along the reaction coordinate. In order to ascertain whether this is a true maximum along the reaction pathway, a calculation for the reverse reaction, *i. e.* the dissociation of diborane into two boranes, was also carried out. It was found that the pathway for the reverse reaction also has the same maximum. However, in the calculation of the third pathway, the maximum along the pathway is not at all obvious. Hence, the transition state is found with the aid of a two-dimensional energy contour map.

#### RESULTS AND DISCUSSION

The MNDO structures of  $BH_3$  and  $B_2H_6$  have  $D_{3h}$  and  $D_{2h}$  symmetries, respectively. The MNDO structures of these two species are illustrated in Figure 2, along with the experimental findings<sup>7</sup> for  $B_2H_6$ . As can be seen from this figure, the agreement between the MNDO and experimental results is

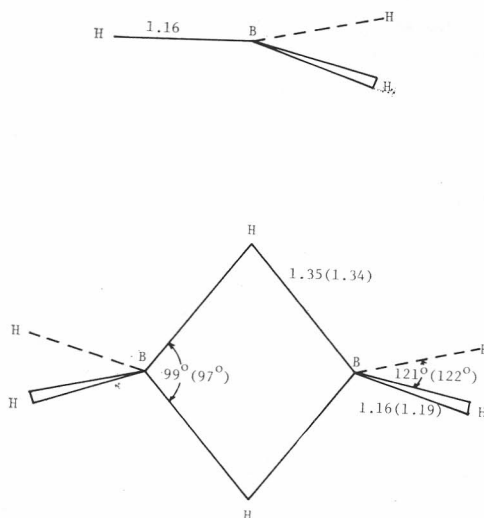


Figure 2. MNDO structures of BH<sub>3</sub> ( $D_{3h}$  symmetry) and B<sub>2</sub>H<sub>6</sub> ( $D_{2h}$  symmetry). Bond lengths are in Å. Values in brackets are experimental results.

very good. Also, the MNDO results are in good agreement with those of Lipscomb<sup>8</sup>, using RH and PRDDO (with extensive configuration interaction) methods.

The MNDO heats of formation of BH<sub>3</sub> and B<sub>2</sub>H<sub>6</sub> are 11.7 and -1.8 kcal/mol, respectively, yielding a heat of dimerization of -25.2 kcal. This deviates somewhat from the experimental value<sup>1,2</sup> of about -35 kcal. However, the MNDO result is still better than the PRDDO value of -17 kcal, as calculated by Lipscomb.<sup>8</sup> Finally, it is noted that the empirical fitting process by Wade<sup>9</sup> gives an excellent estimate, -33.8 kcal, for the dimerization energy.

More recently, applying many-body perturbation theory, Redmon *et al.*<sup>10</sup> have obtained a binding energy of 35 kcal/mol for diborane, with correlation effects accounting for 48% of the binding. Also, applying generalized molecular orbital theory, Taylor and Hall<sup>11</sup> have concluded that there is a substantial effect of electron correlation on the bonding of diborane.

The three dimerization pathways are now discussed in detail.

### The $C_{2h}$ Pathway

The energy profile of this pathway is shown in Figure 3. From this figure it can be seen that the activation energy for the pathway is 3.8 kcal/mol, in fair agreement with that obtained by Lipscomb<sup>8</sup>, 2.6 kcal/mol.

The course of reaction can be understood by considering the correlation diagram shown in Figure 4 between two BH<sub>3</sub> units and the dimer B<sub>2</sub>H<sub>6</sub>. The six bonding orbitals change their orbital energies as the two BH<sub>3</sub> units approach each other. The  $1a_g$  orbital, which has the lowest energy, is stabilized appreciably by a B-B  $\sigma$  overlap. This is a bonding orbital for the whole skeleton but it is mainly localized among the two boron atoms and the two bridging hydrogens. The next orbital,  $1b_u$ , rises in energy due to the out-of-phase inter-

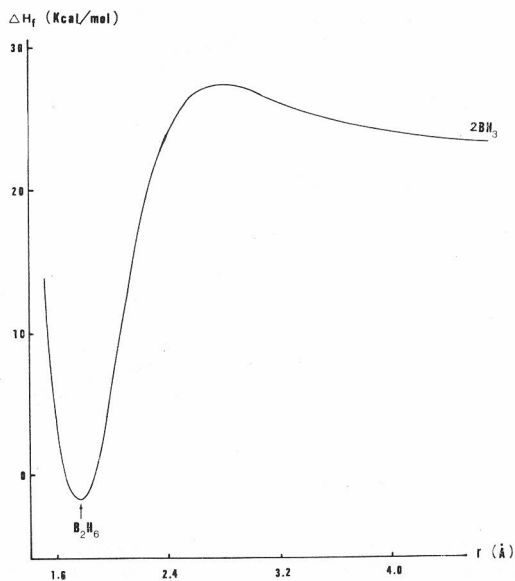


Figure 3. The energy profile for the dimerization of  $\text{BH}_3$  by the pathway with  $C_{2h}$  symmetry.

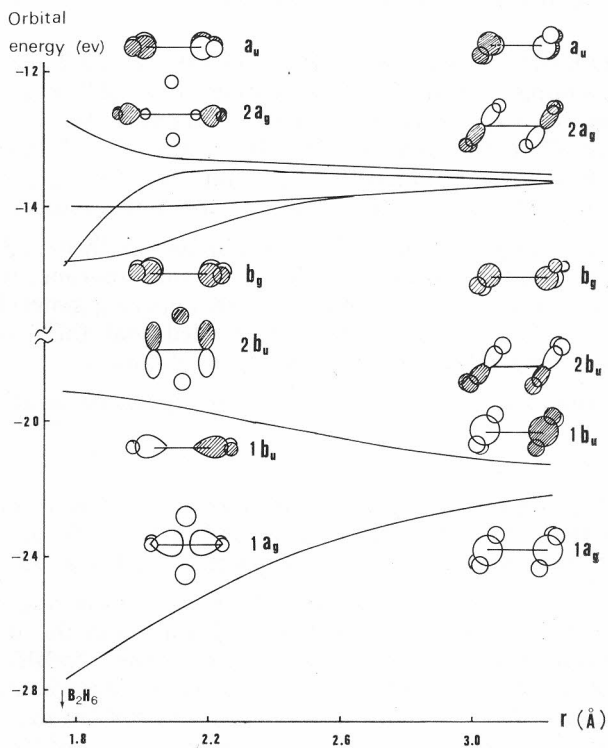


Figure 4. Correlation diagram between two  $\text{BH}_3$  units and  $\text{B}_2\text{H}_6$  for the  $C_{2h}$  pathway.

action between the boron atoms. This is a bonding orbital for the borons and their terminal hydrogens. The third orbital,  $2b_u$ , like the  $1a_g$  orbital, has bonding interaction among the borons and the bridging hydrogens. The difference between  $1a_g$  and  $2b_u$  is that the overlap between the borons is of  $\sigma$  symmetry in the former and  $\pi$  symmetry in the latter. Thus, according to these results, it can be seen that the bonds between the borons and the bridging hydrogens are fairly strong. The fourth orbital,  $b_g$ , is higher in energy than  $2b_u$  by a very minute amount. It bonds the terminal hydrogens to the borons and the overlap between the two borons is of  $\pi$  symmetry. The last two orbitals are bonding orbitals mainly for terminal hydrogens and the boron atoms, with the HOMO being antibonding between the borons. As a consequence, if  $H_2B_6$  is ionized to  $B_2H_6^+$ , the bonding between borons and their terminal hydrogens will be weakened, while the boron-boron bond and those between the borons and the bridging hydrogens will be strengthened.

Returning to Figure 3, in the region  $r > 2.78 \text{ \AA}$ , energy rises smoothly to reach the transition state, whose geometry is shown in Figure 5. At the transition state the interaction between the two  $BH_3$  units is still relatively weak since the shortest distance between the two  $BH_3$  units is  $2.31 \text{ \AA}$ , which is the separation between  $H_3$  and  $B_1$ . The small rise in energy at the transition state may be due to the core-core repulsion between the two boron atoms. Also, the charge distribution remains practically unaltered when the transition state is

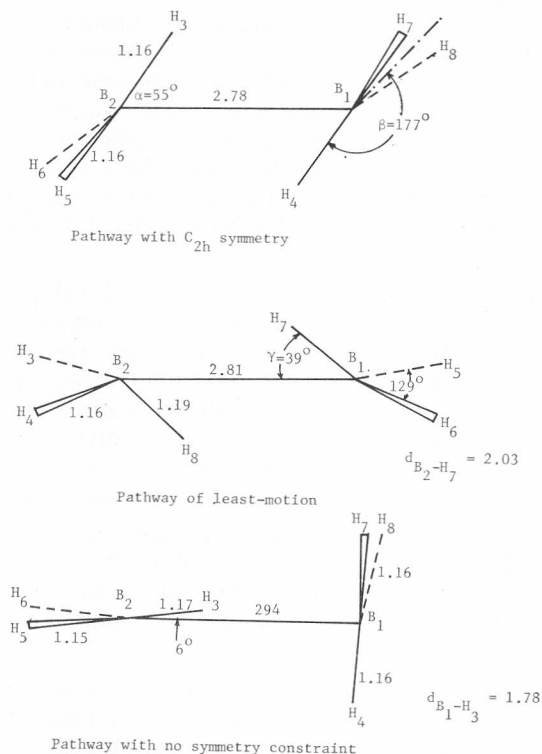


Figure 5. Transition state geometries for the three dimerization pathways of borane. Bond lengths are in  $\text{\AA}$ .

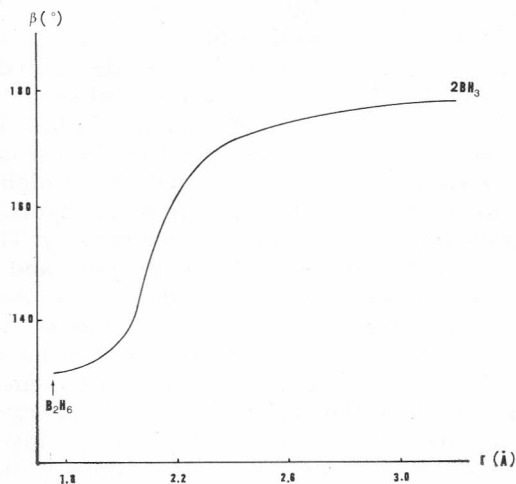


Figure 6. The change of bending angle  $\beta$  along the reaction pathway with  $C_{2v}$  symmetry.

reached. The bending of each  $BH_3$  unit, defined by the bending angle  $\beta$  (see Figure 1), is of interest. The change in this angle throughout the path is shown in Figure 6. At the transition state  $\beta$  is  $177^\circ$ , almost equal to that for the planar  $BH_3$  unit. The bond  $H_4-B_1$ , which will become part of a three-center bond with  $B_2$ , remains virtually unchanged. The angle  $\alpha$  fluctuates in the range of  $54-62^\circ$  before the transition state is reached. At the initial stage of dimerization an increase in  $\alpha$  is expected since there is repulsion between  $H_3$  and  $H_4$ . As the two  $BH_3$  units approach each other a decrease in  $\alpha$  results. This is due to the interaction between the hydrogens  $H_3$  and  $H_4$  with the empty boron  $p$  orbitals.

Beyond the transition state, at  $r \sim 2.1 \text{ \AA}$ , the bond order of  $H_4-B_1$  decreases and that of  $H_4-B_2$  increases. This indicates the formation of the three-center bonds. It is noted that the sum of these two bond orders remains constant throughout the reaction path. However, the bond order between the borons increases markedly after the transition state is reached. Hence, according to these results, the stability of  $B_2H_6$  over two  $BH_3$  units is not due to the formation of the three-center banana bonds. Rather, it is due to the boron-boron interaction. This can also be seen from the correlation diagram of Figure 4.

After the transition state ( $r = 2.78 \text{ \AA}$ ) is reached, there is a steady flow of electrons toward the borons. In the range of  $2.10 \text{ \AA} < r < 2.78 \text{ \AA}$ , the sources of the electrons are the terminal hydrogens. For the range of  $r < 2.10 \text{ \AA}$ , the bridging hydrogens become the electron source, as the three-center bonds start to form.

The formation of the three-center bonds is also evident when the changing pattern of the bending angle  $\beta$  is examined. In the range  $2.0 \text{ \AA} < r < 2.2 \text{ \AA}$  there is a dramatic decrease in  $\beta$ , indicating that the three-center bonds are being formed. Also in this range angle  $\alpha$  decreases steadily to a minimum of  $43.4^\circ$  at  $r = 2.0 \text{ \AA}$ . At this point the two bridging hydrogens are nearly

midway between the borons. When diborane is finally formed at  $r = 1.75 \text{ \AA}$ ,  $\alpha$  increases back to  $49.5^\circ$ .

Roughly speaking, this dimerization process proceeds in two stages. The first stage is concerned with the increase in boron-boron interaction. The second stage is the formation of B—H—B three-center bonds. The first stage starts at  $r = 2.78 \text{ \AA}$  and is almost finished at  $r = 2.10 \text{ \AA}$ . The second stage does not become important until  $r$  reaches  $2.10 \text{ \AA}$ .

### The Least-Motion Pathway

The energy profile of this pathway, shown in Figure 7, as expected, gives a high energy barrier for dimerization. The activation energy determined is  $31.5 \text{ kcal/mol}$ . Such a large activation energy is due to the confinement of the four terminal hydrogens and the borons to stay co-planar. On the other hand, quite accidentally, the transition state of this path has a boron-boron separation of  $2.81 \text{ \AA}$ , nearly the same as that for the previous path. The transition state geometry for the least-motion pathway is shown in Figure 5.

For the region  $r > 2.81 \text{ \AA}$ , the approaching of the hydrogens  $H_7$  and  $H_8$  makes the energy rise smoothly and enormously to reach the transition state. To release the repulsion between them,  $H_7$  and  $H_8$  come out of the plane, thus bending the  $BH_3$  units. The angle  $\gamma$  (see Figure 1), which indicates the degree of non-planarity of the  $BH_3$  units, increases correspondingly to a value of  $39.4^\circ$  at the transition state. Also, at this point, the attraction interaction between the  $BH_3$  units is relatively weak as atoms  $H_7$  and  $B_2$  are still  $2.03 \text{ \AA}$  apart. In other words, no significant three-center bond has been formed at this stage. Also, in this region, there is an electron flow from the terminal hydrogens through their respective borons to the bridging hydrogens.

In the region  $2.30 \text{ \AA} < r < 2.81 \text{ \AA}$  the energy drops rapidly as a consequence of the formation of the three-center bonds and the concomitant increase of boron-boron interaction. In the initial stage of this region the bending angle  $\gamma$  increases slightly then falls to  $36.9^\circ$  at  $r = 2.30 \text{ \AA}$ . The increase in  $\gamma$  shows that the repulsion of the two hydrogens,  $H_7$  and  $H_8$ , is still significant. At  $r = 2.30 \text{ \AA}$  these hydrogens have shifted to the center positions, *i. e.*, three-

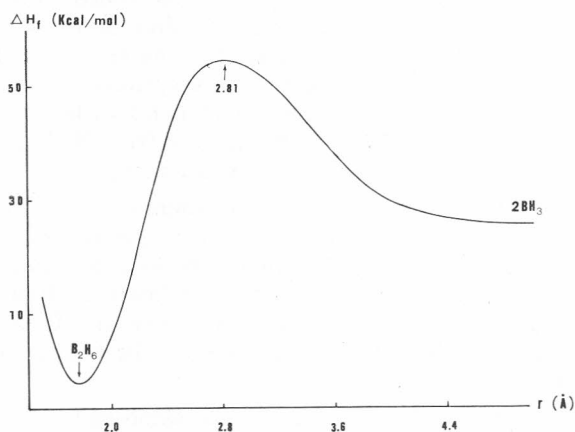


Figure 7. The energy profile for the dimerization of  $BH_3$  by the least-motion pathway.

-center bonds have been formed. It is noted that in this path the three-center bonds are formed at an earlier stage,  $r = 2.30 \text{ \AA}$ , than in the previous path,  $r = 2.10 \text{ \AA}$ . Since the terminal hydrogens and the borons are kept to be co-planar throughout this path, earlier formation of the three-center bonds would release the »bending strain« around the borons. In this region charges flow from the terminal hydrogens to the borons and the bridging hydrogens. This again is indicative of the formation of the three-center bonds and boron-boron interaction.

In the region of  $r < 2.30 \text{ \AA}$ , energy drops to a minimum of  $-1.8 \text{ kcal/mol}$  to form diborane. The bending angle  $\gamma$  increases to  $49.5^\circ$  for diborane as the borons approach each other. Also, the charges on the terminal hydrogens remain practically unchanged in this region, but there is a steady flow of charge from the bridging hydrogens to the borons. This electron flow serves to strengthen the formation of the three-center bonds.

#### *The Pathway with No Symmetry Constraint*

The energy profile of this pathway is shown in Figure 8. In this figure the transition state cannot be found readily due to the flat energy plateau. Thus, a two-dimensional energy contour map, as shown in Figure 9, is constructed to locate the transition state. As expected, the region around the transition state shows very little variation in energy. Hence the location of the transition state is far from obvious and the one we have determined must be viewed with caution. The transition state geometry is again shown in Figure 5.

For the region  $r > 3.20 \text{ \AA}$ , energy rises from  $23.5 \text{ kcal/mol}$  to  $26.1 \text{ kcal/mol}$ , which is very close to the transition state energy, namely,  $26.2 \text{ kcal/mol}$ . In this region the angle  $\delta$  (see Figure 1) remains close to  $0^\circ$ , *i. e.*, the bond  $B_2-H_3$  is pointing directly to the empty  $p$  orbital of  $B_1$ . At  $r = 3.20 \text{ \AA}$ , the interaction between  $B_1$  and  $H_3$  is still rather weak for their separation which is  $2.04 \text{ \AA}$ . Electron flow from  $B_2$  to  $B_1$  through  $H_3$  is observable, though the amount, about  $0.02e$ , is small. Charges on atoms remain unchanged.

As  $r$  continues to shorten the energy remains almost unchanged till  $r = 2.70 \text{ \AA}$ . At this point the energy is equal to that at  $r = 3.20 \text{ \AA}$ , but is  $0.1 \text{ kcal/mol}$  lower than the transition state energy, as shown in Figure 8. Even though the energy change in this region is exceptionally small, the angle  $\delta$  increases rapidly from about  $0^\circ$  to  $22.6^\circ$ . The bond order between  $H_3$  to  $B_1$  increases by a small amount, but the electron flow from  $B_2$  to  $B_1$  is large, while the charges on all the hydrogens are nearly unchanged.

For the region  $2.31 \text{ \AA} < r < 2.70 \text{ \AA}$  the energy is on the decrease. The angle  $\delta$  increases dramatically to  $49.3^\circ$  while the angle  $H_4-B_1-B_2$  decreases to the same value. The  $B_1-H_3$  separation increases to a maximum of  $1.79 \text{ \AA}$  as a consequence of the increase in  $\delta$ . Charge continues to flow from  $B_2$  to  $B_1$  until the two charges become equal. Needless to say, the flow back of charge is through  $H_4$ . It is noted that so far the changes in charge densities on the other hydrogens are negligible.

For the region of  $r < 2.31 \text{ \AA}$  the path is the same as the  $C_{2h}$  path discussed previously. Again, at  $r = 2.00 \text{ \AA}$  the bridging hydrogens become equidistant between the two borons and act as electron sources for the formation of the



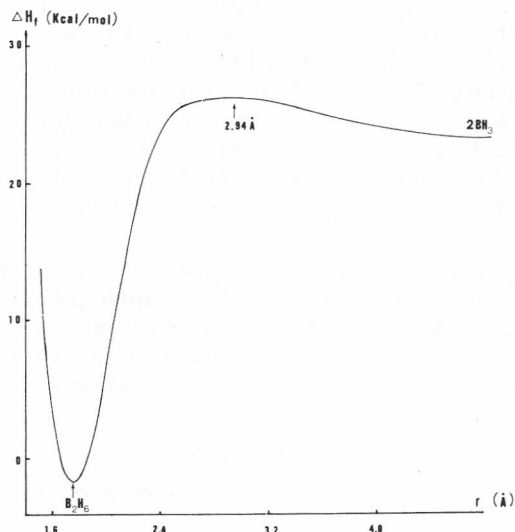


Figure 8. The energy profile for the dimerization of  $\text{BH}_3$  by the pathway with no symmetry constraint.

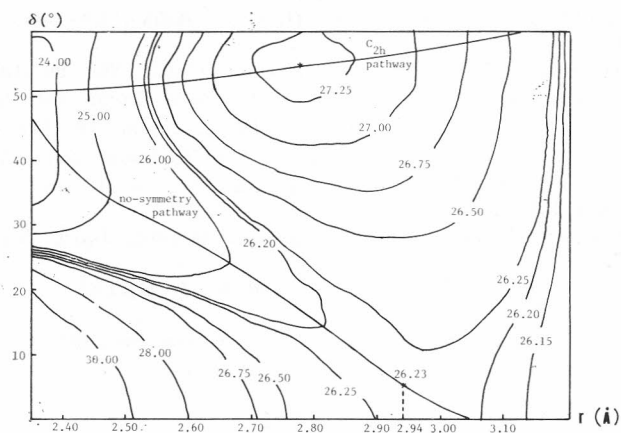


Figure 9. Energy (kcal/mol) contour map for the dimerization pathway with no symmetry constraint. The ordinate is the value of  $\delta$  ( $^\circ$ ) and the abscissa is  $r$ , the B—B separation ( $\text{\AA}$ ). The transition state is indicated by an asterisk. In addition, the  $C_{2h}$  pathway is also shown for reference.

three-center bonds. Energy drops to a minimum at  $r = 1.75 \text{ \AA}$  as diborane is formed. It is noted that even when no symmetry condition is imposed the reaction path retains  $C_s$  symmetry throughout.

#### CONCLUSION

As a consequence of the involvement of an empty valence orbital in the reaction, the dimerization of borane has a transition state with a large boron-boron separation. Another consequence is the low energy barrier for the reaction. Among the paths studied, the path having the lowest barrier is that

with  $C_s$  symmetry. The activation energy for this path is 2.7 kcal/mol. For this path it is rather difficult to locate the transition state since a large rearrangement of atoms brings about a small variation in energy, *i. e.*, the transition state is on a flat surface. Thus it is obvious that the stereochemical requirement for the dimerization is not strictly confined and the dimerization can proceed very efficiently. Furthermore, in view of the known tendency of MNDO to yield high energy for transition states, the low activation energy for the  $C_s$  pathway *probably* means that the dimerization has no or a very small energy barrier.

The  $C_s$  path has been suggested by Gimarc<sup>12</sup> and Fehlnert<sup>2</sup>, but rejected by Lipscomb<sup>8</sup>. According to Lipscomb<sup>8</sup>, the optimal path is the one with  $C_{2h}$  symmetry with an activation energy of 2.6 kcal/mol. This is in very good agreement with our results. Also, when CI is included in his SCF calculation, the transition state occurs at a boron-boron separation of 3.0 Å, in fair agreement with our result.

## REFERENCES

1. L. H. Long, in: *Progress in Inorganic Chemistry*, S. J. Lippard (Ed.), **15** (1972) 1.
2. G. W. Mappes, S. A. Fridmann, and T. P. Fehlnert, *J. Phys. Chem.* **74** (1970) 3307; T. P. Fehlnert and S. A. Fridmann, *Inorg. Chem.* **9** (1970) 2288.
3. W. C. Hamilton, *Proc. Royal Soc. (London)* **A235** (1956) 395; *J. Chem. Phys.* **29** (1958) 460.
4. M. J. S. Dewar and W. Thiel, *J. Amer. Chem. Soc.* **99** (1977) 4899.
5. M. J. S. Dewar and M. L. McKee, *J. Amer. Chem. Soc.* **99** (1977) 5231.
6. M. J. S. Dewar and M. L. McKee, *Inorg. Chem.* **18** (1979) 1312.
7. D. S. Jones and W. N. Lipscomb, *Acta Crystallogr. Sect. A* **26** (1970) 1961.
8. D. A. Dixon, I. M. Pepperberg, and W. N. Lipscomb, *J. Amer. Chem. Soc.* **96** (1974) 1235.
9. C. W. Housecroft, R. Snaith, and K. Wade, *Inorg. Nucl. Chem. Lett.* **15** (1979) 343.
10. L. T. Redmon, G. D. Purvis III, and R. J. Bartlett, *J. Amer. Chem. Soc.* **101** (1979) 2856.
11. T. E. Taylor and M. B. Hall, *J. Amer. Chem. Soc.* **102** (1980) 6136.
12. B. M. Gimarc, *J. Amer. Chem. Soc.* **95** (1973) 1417.

## SAŽETAK

## Studij dimerizacije borana s pomoću MNDO metode

Wing-Kwong Ip i Wai-Kee Li

Razmotrena je dimerizacija borana primjenom semiempirijske MNDO metode. Ispitani su putevi reakcije s nametnutim uvjetima simetrije  $C_{2h}$ , najmanjeg gibanja i simetrije  $C_s$ . Odgovarajuće energije aktivacije jesu: 3,8, 31,5 i 2,7 kcal/mol. Budući da metoda MNDO obično daje previsoke energije prijelaznih struktura (TS), niska vrijednost za simetriju  $C_s$  upućuje na zaključak da je energija aktivacije izuzetno mala ili čak jednaka nuli.